SCIENCE CHINA
Chemistry

• ARTICLES •

May 2014 Vol.57 No.5: 739–747
doi: 10.1007/s11426-013-5027-1

Carbon-supported Fe/Co-N electrocatalysts synthesized through heat treatment of Fe/Co-doped polypyrrole-polyaniline composites for oxygen reduction reaction

YI QingFeng[1*], ZHANG YuHui[1], LIU XiaoPing[1] & YANG YaHui[2*]

[1]*School of Chemistry and Chemical Engineering, Hunan University of Science and Technology, Xiangtan 411201, China*
[2]*College of Resource and Environment, Hunan Agricultural University, Changsha 410128, China*

Received July 3, 2013; accepted September 18, 2013; published online December 4, 2013

In this paper, we synthesized cathode catalysts (PANI-PPYR, Fe/PANI-PPYR, Co/PANI-PPYR and Fe-Co/PANI-PPYR) with high performance oxygen reduction by using a simple heat treatment process. These catalysts were fabricated by directly calcining the Fe and/or Co doped polyaniline (PANI)-polypyrrole (PPYR) composites. Their electrocatalytic activity for ORR both in acidic and in alkaline media was investigated by voltammetric techniques. Among the prepared catalysts, Co/PANI-PPYR presents the most positive ORR onset potential of 0.62 V (vs. SCE) in 0.5 mol/L H_2SO_4 solution or –0.09 V (vs. SCE) in 1 mol/L NaOH solution. In addition, the Co/PANI-PPYR catalyst shows the largest limiting-diffusion current density for ORR, which is 4.3 mA/cm^2@0.2 V (vs. SCE) in acidic and 2.3 mA/cm^2@–0.3 V (vs. SCE) in alkaline media. In acidic media, a four-electron reaction of ORR on the Co/PANI-PPYR and Fe/PANI-PPYR catalysts is more dominant than a two-electron reaction. In alkaline media, however, a four-electron and a two-electron mechanisms are co-present for the ORR on all the prepared catalysts. Co/PANI-PPYR catalyst also presents good electrocatalytic activity stability for ORR both in acidic and in alkaline media.

oxygen reduction reaction, polyaniline, polypyrrole, fuel cells

1 Introduction

Oxygen reduction reaction (ORR) is the cathodic reaction of polymer electrolyte membrane fuel cells (PEMFCs). However, the sluggish kinetics of the ORR significantly hinders the performance of the PEMFCs. Although platinum and Pt-based catalysts display excellent electrocatalytic activity for ORR in acidic and alkaline media, the high cost of Pt limits their practical application and therefore, development of non-platinised composite electrocatalysts used for ORR represents a meaningful and necessary alternative. Much attention has been paid to the study on metal macromolecules containing nitrogen used as electrocatalysts for ORR due to Jasinski's report in 1964 [1]. Although the transition metal macromolecules displayed good electroactivity for ORR [2, 3], they showed poor electrocatalytic stabiliy in acidic media. Further investigation showed that the electroactivity and stability of the transition metal macromolecules catalysts got significant improvement after they were subjected to the heat treatment under inert gas atmosphere [4]. In addition, transition metal carbon-nitrogen composites have also been paid extensive attention as efficient non-precious metal ORR electrocatalysts [5–7]. Much progress has been made on the preparation of Fe/(or Co)-C-N composites for ORR. Nitrogen-containing carbon nanofiber (CN_x) catalysts grown by acetonitrile pyrolysis over 2 wt% Fe, Co, and Ni were prepared by Biddinger and Ozkan [8] and these catalysts showed no methanol poisoning during ORR. Liu [9] *et al.* reported the synthesis of N-doped or-

*Corresponding authors (email: yqfyy2001@hnust.edu.cn; yangyahui2002@sina.com)

dered porous carbon (CN_x) via a nano-casting process using polyacrylonitrile (PAN) as the carbon and nitrogen precursor. This CN_x catalyst presented high onset potential and large current density for ORR. A highly ordered Pt-free Fe-N-C catalyst was prepared through a hydrogen bonding-assisted, self-assembly route [10]. Cells assembled with this Fe-N-C catalyst perform significantly better than those assembled with amorphous Fe-N-C cathode catalysts. Carbon nanotubes (CNTs) exhibit unique surface characteristics and have been extensively used as the carbon support to synthesize the Fe (or Co) and N-doped C-N composites, which presented high electroactivity and good stability for ORR [11–13]. Recently, Wu *et al*. [14] reported their much meaningful work on the preparation of the ORR electrocatalysts derived from polyaniline, iron, and cobalt. They found that these catalysts presented high performance for ORR and the most active materials in the group catalyzed the ORR at potentials within ~60 mV of that delivered by state-of-the-art Pt/C. Both polyaniline (PANI) and polypyrrole (PPYR) are solid polymers containing C, H and N, and can be used as precursors of C-N compound catalysts. According to the ORR mechanism on the transmit metals doped C-N composite catalysts [15–19], the doped transition metals played significant role in the electroactivity of the C-N compound catalysts for ORR. In this work, we firstly carried out the polymerization of aniline and pyrrole in the presence of iron and cobalt salts to synthesize the Fe/Co doped polyaniline (PANI)-polypyrrole (PPYR) composites. Then they were subjected to high temperature treatment to obtain the preliminary catalysts. The preliminary catalysts were subsequently leached in sulfuric acid solution to remove the soluble impurities. The as-obtained samples were finally heated to a high temperature again to synthesize the metal doped C-N catalysts. Their morphological structure was characterized by scanning electron microscopy (SEM) and their electroactivity for ORR in acidic and alkaline media was studied by voltammetric techniques. Compared with the references, the Fe/Co doped PANI-PPRY catalyst in this work were prepared without the use of other carbon materials like the commercial carbon powder [14] and carbon nanotubes [11–13], and the metal macromolecules [1–4]. This results in the low cost and simple preparation process of the catalysts of the present investigation.

2 Experimental

2.1 Catalyst synthesis and physical characterization

Aniline, pyrrole, ammonium persulfide ($(NH_4)_2S_2O_8$), iron chloride ($FeCl_3\cdot 6H_2O$), cobalt nitrate ($Co(NO_3)_2\cdot 6H_2O$), hydrochloric acid (HCl, 35%), sodium hydroxide (NaOH, 98%), and Pt/C (20%) all procured from Sinopharm Group Chemical Regent Co. Ltd. were used in the catalysts preparation. Pure water (18.2 Ω cm) was obtained from doubly distilled water that has been subjected to the treatment of ion exchange resins.

Four catalysts, PANI-PPYR, Fe/PANI-PPYR, Co/PANI-PPYR and Fe-Co/PANI-PPYR, were prepared according to the following process.

PANI-PPYR

Firstly, 0.36 mL pyrrole was dissolved in 30 mL H_2O to form the solution A. 1.14 g $(NH_4)_2S_2O_8$ was dissolved in 10 mL H_2O to form the solution B. A and B were then mixed, and the mixture solution was held on at 6 °C for 24 h to obtain the mixture C containing the polypyrrole. 0.36 mL aniline and 1.14 g $(NH_4)_2S_2O_8$ were then added to the mixture C under stirring. After the as-formed mixture was held on at 20 °C for 24 h, the water and other un-reacted organic materials in the mixture were removed under vacuum through a rotary evaporator. The wet solid particles were subsequently dried at 40 °C over night in a vacuum oven to obtain the catalyst precursor. The precursor was transferred to a tube furnace and then the tube furnace was heated up to 350 °C at a rate of 2 °C/min under N_2 atmosphere and held on at 350 °C for 2 h. And then, the tube furnace was continuously heated up to 700 °C at the same heating rate under N_2 atmosphere and held on at 700 °C for 2 h. After cooling down, the collected powder was acid-leached in 0.5 mol/L H_2SO_4 at 80 °C for 8 h and then thoroughly washed by water. After dried at 40 °C over night in a vacuum oven, the resulting powder was transferred to a tube furnace again. The tube furnace was heated up to 900 °C at a rate of 4 °C/min, and then allowed to cool down from 900 °C to the room temperature. The powder thus obtained was the catalyst marked by PANI-PPYR.

Fe/PANI-PPYR

Preparation procedure of the Fe/PANI-PPYR catalyst was the same as the PANI-PPYR except for the solution B. For the Fe/PANI-PPYR, the solution B was obtained by the dissolution of 1.14 g $(NH_4)_2S_2O_8$ and 0.13g $FeCl_3\cdot 6H_2O$ in 10 mL H_2O. The powder finally obtained was marked by Fe/PANI-PPYR

Co/PANI-PPYR

Preparation procedure of the Co/PANI-PPYR catalyst was the same as the PANI-PPYR except for the solution B. For the Co/PANI-PPYR, the solution B was obtained by the dissolution of 1.14 g $(NH_4)_2S_2O_8$ and 0.15 g $Co(NO_3)_2\cdot 6H_2O$ in 10 mL H_2O. The powder finally obtained was marked by Co/PANI-PPYR.

Fe-Co/PANI-PPYR

Preparation procedure of the Fe-Co/PANI-PPYR catalyst was the same as the PANI-PPYR except for the solution B. For the Fe-Co/PANI-PPYR, the solution B was obtained by the dissolution of 1.14 g $(NH_4)_2S_2O_8$, 0.065 g $FeCl_3\cdot 6H_2O$,

and 0.075 g $Co(NO_3)_2 \cdot 6H_2O$ in 10 mL H_2O. The powder finally obtained was marked by Fe-Co/PANI-PPYR.

physical characterization

Scanning electron microscopy (SEM) images of the catalysts were recorded using a field emission scanning electron microscope (Nova NanoSEM230). Metal (Fe and Co) contents of the samples were determined by their energy dispersive spectra (EDS), where Ti plates were used as the substrates loading the sample particles. Transmission electron microscopy (TEM) images were taken on a Philips EM420 microscope. Phases present in the catalysts were identified by powder X-ray diffraction (XRD) analysis (Ultima IV Multipurpose X-Ray Diffraction System, Cu-Ka). Elemental nitrogen (N) content of the samples was obtained by the X-ray photoelectron spectroscopy (XPS) technique (K-Alpha 1063).

2.2 Electrode preparation and electrochemical characterization

Working electrodes were fabricated by the following procedure. 5 mg of catalyst particles, 1 mL ethanol and 50 μL of Nafion solution (5 wt% solution) were mixted and the mixture was sonicated for 30 min in an ultrasonicator to get a fine dispersion of catalyst particles (called catalyst ink). A measured volume of the ink was transferred using a micropipette onto a polished glassy-carbon disk electrode (4 mm diameter). The electrode was dried at room temperature to get a thin film of the catalyst on the glassy-carbon disk, which was used as the working electrode in electrochemical measurements. The loading of the catalysts and the commercial Pt/C on the glassy-carbon disk was 0.59 mg/cm^2.

Electrochemical measurements were carried out with a computer-controlled AutoLab PGSTAT30/FRA electrochemical system using a conventional three-electrode system, which consisted of a working electrode (the prepared samples), a platinum foil counter electrode and a saturated calomel electrode (SCE) as a reference electrode. All potentials in the paper were reported versus SCE. Prior to electrochemical experiments, the working electrode was cleaned in N_2 saturated 1 mol/L NaOH (or 0.5 mol/L H_2SO_4) solution by repeatedly cycling the potential from –0.3 V to 1.0 V (or –0.8 V to 0.5 V) at a scan rate of 100 mV/s until reproducible cyclic voltammograms (CVs) were obtained. The oxygen reduction measurements were carried out using a rotating disk electrode (RDE) in O_2-saturated electrolyte solutions. All electrochemical experiments were carried out in ambient temperature (20 ± 2 °C).

3 Results and discussion

Morphological structure of the prepared catalysts was examined by scanning electron microscopy (SEM). As seen in Figure 1, the particles of the prepared catalysts are interconnected to form a porous structure. In addition, a part of particles of the Fe/PANI-PPYR catalyst were aggregated. However, the particle sizes of the prepared catalysts are different. Figure 1(a, c) shows that the PANI-PPYR and Co/PANI-PPYR catalysts display the large particle sizes of 380–560 and 380–660 nm, respectively. Fe/PANI-PPYR and Fe-Co/ PANI-PPYR catalysts present approximately the same particle sizes of 220–330 and 220–380 nm, respectively, as shown in Figure 1(b, d). The results indicate that the addition of various metals has an impact on the morphological structure of the PANI-PPYR catalyst. Although the particles of the Fe/PANI-PPYR and Fe-Co/PANI-PPYR catalysts exhibit the smallest sizes among the prepared four samples, they don't show the best performance of ORR as indicated in Figure 6. This shows that the surface area of the catalysts obtained from Fe/Co-doped PANI-PPYR composites doesn't play the most key role on their electrocatalytic activity for ORR.

The texture of particles was further examined by TEM technique. Figure 2(A) shows that the PANI-PPYR catalyst is mainly composed of short fiber-like tubes with a diameter of 7 nm (the inset (a) of Figure 2(A)). A small number of particles with the size of ca. 23 nm are present in the inset (b) of Figure 2(A). However, the short fibrous tubes are not found on other catalysts (Figure 2(B–D)), showing that the structure of the PANI-PPYR is broken down in the presence of metal salts. In addition, particles of the Fe/PANI-PPYR catalyst are massive as shown in Figure 2(B), resulting in the decrease of its real surface area. This massive structure is also observed on the Fe-Co/PANI-PPYR (Figure 2(D)). Figure 2(C) and its inset show that the particles of the Co/PANI-PPYR display a different structure, which is composed of smaller sizes of particles. This would be favorable for the formation of more active sites.

Figure 3 shows the XRD patterns of the prepared catalysts. As shown in Figure 3, two wide diffraction peaks, located at 24.4–25.4 and 43.6, can be observed on the all

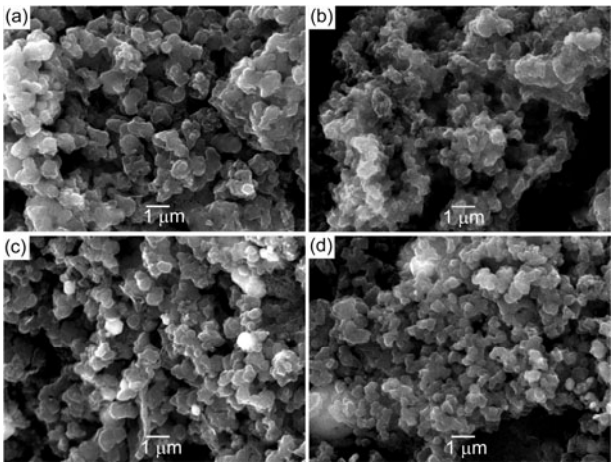

Figure 1 SEM images of PANI-PPYR (a), Fe/PANI-PPYR (b), Co/PANI-PPYR (c) and Fe-Co/PANI-PPYR (d).

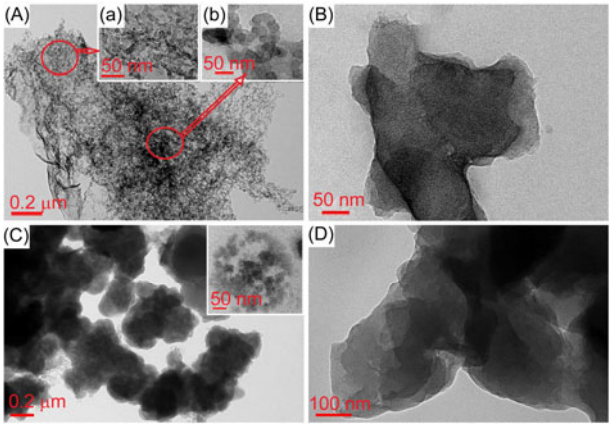

Figure 2 TEM images of PANI-PPYR (A), Fe/PANI-PPYR (B), Co/PANI-PPYR (C) and Fe-Co/PANI-PPYR (D).

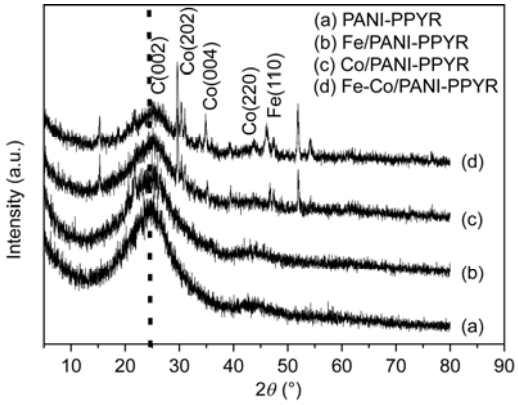

Figure 3 XRD patterns of PANI-PPYR (a), Fe/PANI-PPYR (b), Co/PANI-PPYR (c) and Fe-Co/PANI-PPYR (d).

four catalysts, corresponding to (0 0 2) and (1 0 1) diffractions of graphitic carbon. Compared to the metal-free PANI-PPYR catalyst, other catalysts containing metals (Fe/PANI-PPYR, Co/PANI-PPYR and Fe-Co/PANI-PPYR) show a slightly positive shift in the (0 0 2) peak. This is partially ascribed to a better graphitic crystalline structure caused by the addition of the metal Fe and Co [20]. The small peak at the 2θ value of 43.9° for the Fe/PANI-PPYR and Fe-Co/PANI-PPYR catalysts can be attributed to the bulk of carbidic-state Fe and the formation of α-Fe which have been proved to display ORR electrocatalytic activity [10]. The diffraction peaks at 29.7°, 34.8° and 43.9° arise for the Co/PANI-PPYR and Fe-Co/PANI-PPYR catalysts, which are attributed to the (202), (004) and (220) crystal planes of Co, respectively. The (110) crystal plane of Fe is observed at the 2θ value of 45.9° for Fe/PANI-PPYR and Fe-Co/ PANI-PPYR catalysts. No obvious diffraction peak can be attributed to the Fe-Co alloy phase for the Fe-Co/PANI-PPYR catalyst.

Energy dispersed spectra (EDS) of these samples (Figure 4) indicate a characteristic energy peak at 6.4 keV for Fe, and an energy peak at 6.9 keV for Co. The characteristic peak at 2.3 displays the presence of S in the samples. Mass percentages of Fe and Co in these samples are obtained according to the EDS analysis and listed in Table 1.

Nitrogen elemental content analysis using XPS is shown in Table 1. The N content of the samples follows the order: PANI-PPYR > Fe/PANI-PPYR > Co/PANI-PPYR > Fe-Co/ PANI-PPYR. Considering the important role that nitrogen doping into the carbon structure plays in ORR activity for such type of catalyst, N 1s XPS spectra of the prepared catalysts are compared in Figure 5. Two dominant nitrogen peaks are observed with these catalysts. The peak at 400.7 eV is ascribed to the nitrogen atoms (pyrrolic N) from a pentagon structure [20]. PANI-PPYR, Fe/PANI-PPYR and Fe-Co/ PANI-PPYR catalysts exhibit a N peak at 398.1 eV, which is assigned the pyridinic N. For the Co/PANI-PPYR catalyst, the binding energy of the pyridinic N presents a slight increment (398.3 eV). This favors the nitrogen atoms doped at the edges of the graphitic carbon layers. Therefore, the ORR electroactivity of the Co/PANI-PPYR catalyst is improved [13].

Cyclic voltammograms (CVs) of the prepared catalysts measured at a scan rate of 50 mV/s in a 0.5 mol/L H_2SO_4 solution saturated with respective N_2 and O_2 are shown in Figure 6. Compared to the CVs in the N_2-saturated H_2SO_4 solution, the CVs in the O_2-saturated H_2SO_4 solution exhibit much larger anodic and cathodic current densities. This shows that the as-synthesized catalysts display sensitive responses for the electrochemical behavior of O_2. It is further found from Figure 6(c) that the Co/ PANI-PPYR catalyst presents the largest cathodic current density in O_2-saturated

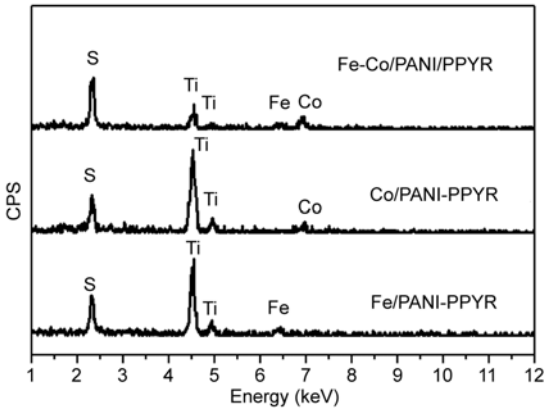

Figure 4 Energy dispersed spectra (EDS) of the samples. Ti peaks are caused by the Ti substrate.

Table 1 Mass percentages of Fe and Co obtained from EDS and N obtained from XPS in the samples

	PANI-PPYR	Fe/PANI-PPYR	Co/PANI-PPYR	Fe-Co/PANI-PPYR
Fe	0	3.48	0	1.38
Co	0	0	4.22	2.58
N	12.07	9.05	8.93	7.39

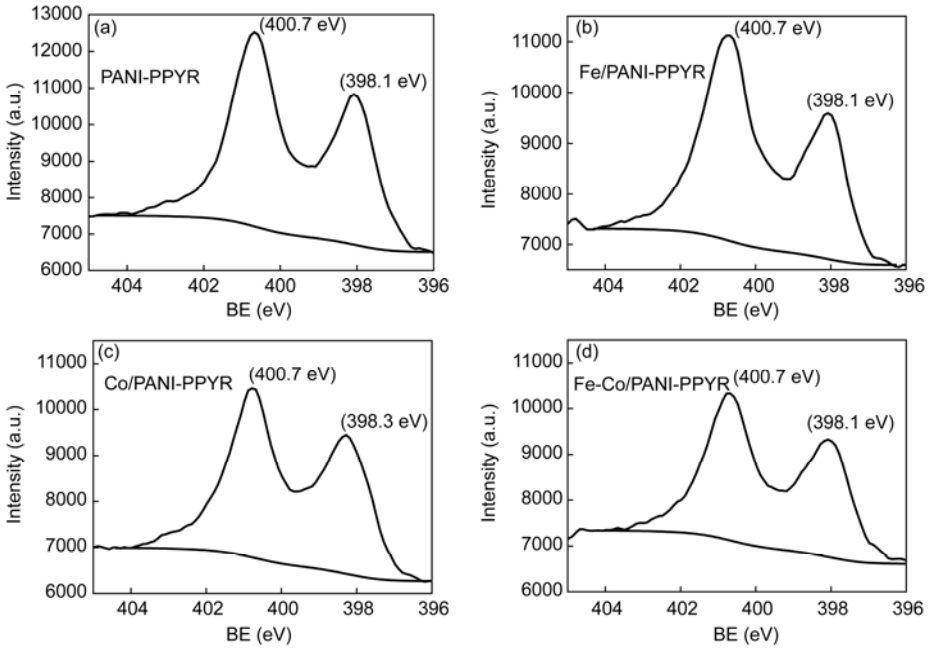

Figure 5 N 1s XPS spectra for the prepared catalysts.

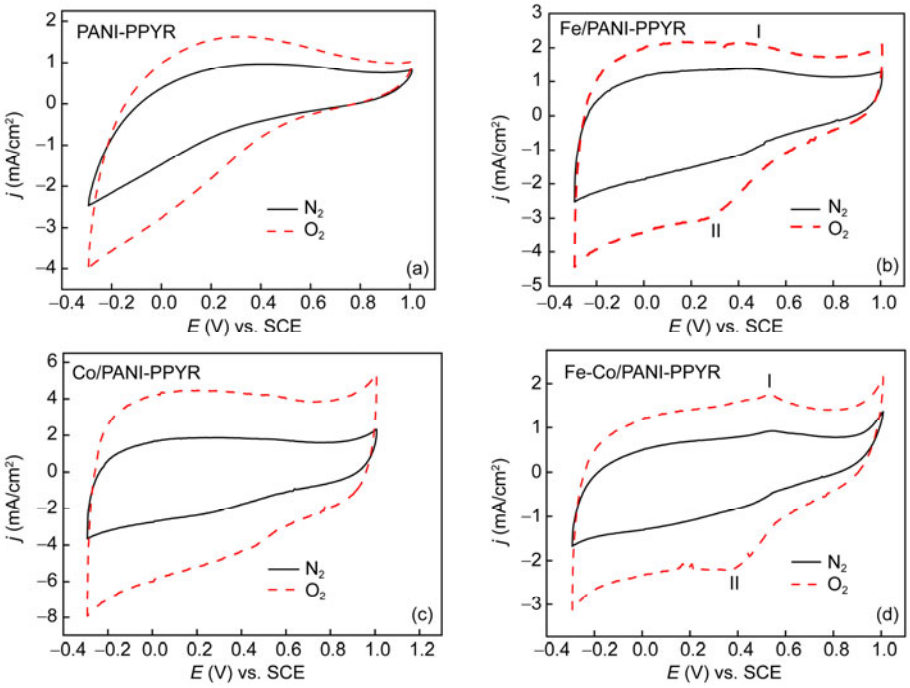

Figure 6 Cyclic voltammograms of the samples in 0.5 mol/L H_2SO_4 solution saturated with N_2 (solid line) and O_2 (dashed line) at a scan rate of 50 mV/s.

H_2SO_4 solution, showing the significantly high electrocatalytic activity of the Co/PANI-PPYR for ORR. Figure 6(b, d) shows that a redox couple develops on the Fe/PANI-PPYR and Fe-Co/PANI-PPYR catalysts, corresponding to the anodic peak I and the cathodic peak II. The cathodic peak II becomes more well-defined in the O_2-saturated electrolyte, which is caused by the oxygen reduction.

In a 1 mol/L NaOH solution, the CV profiles of the prepared samples in O_2-saturated solution are close to those in N_2-saturated solution except for the cathodic current density during the negative-going scan, as shown in Figure 7. The current density on the positive-going scan remains almost unchanged either in N_2-saturated or O_2-saturated solution. This shows that the presence of O_2 doesn't have effect on

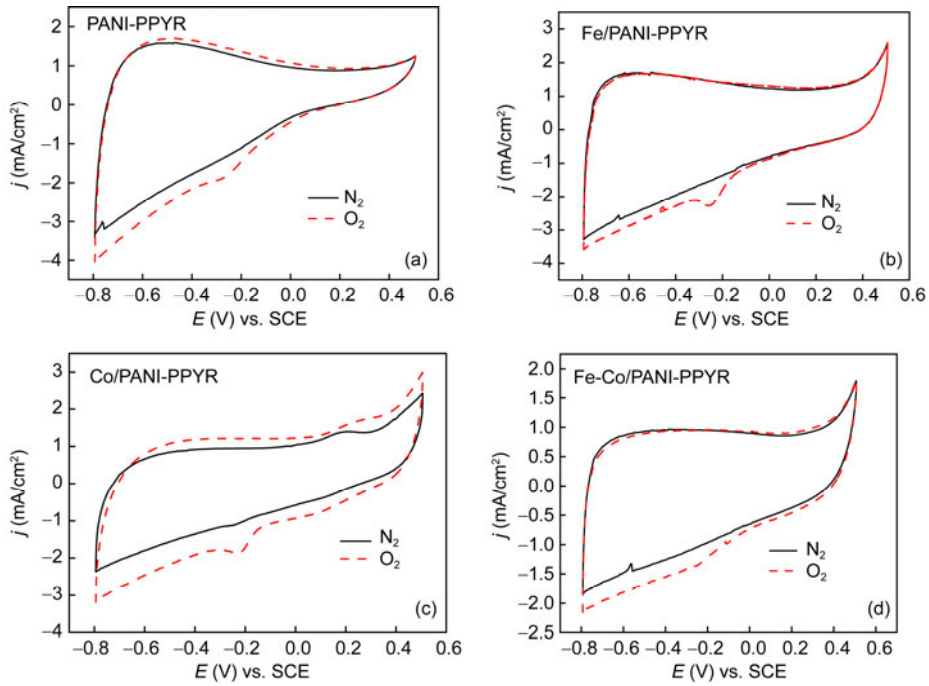

Figure 7 Cyclic voltammograms of the samples in 1 mol/L NaOH solution saturated with N_2 (solid line) and O_2 (dashed line) at a scan rate of 50 mV/s.

the anodic process of the catalysts in alkaline media. The cathodic current density on the positive-going scan presents an increment in O_2-saturated solution, which is caused by the reduction of oxygen.

Figure 8 shows the polarization curve for oxygen reduction on the as-synthesized catalysts in 0.5 mol/L H_2SO_4 and 1 mol/L NaOH solutions. As shown in Figure 8, compared to other three catalysts, the Co/PANI-PPYR catalyst exhibits a significant activity toward oxygen reduction with a relatively smooth diffusion current either in acidic or alkaline media. The onset potential for ORR on the Co/PANI-PPYR catalyst is 0.60 V (vs. SCE) in acidic solution, which is higher than those of PANI-PPYR, Fe/PANI-PPYR and Fe-Co/PANI-PPYR catalysts. The low onset potential and small current density for ORR on the Fe-Co/PANI-PPYR catalyst show that the synergistic effect of Fe and Co for ORR is not present. This would be attributed to the absence of the Fe-Co alloy phase shown in Figure 3. In addition, a rapid increase of the ORR current density arises at the potential lower than 0.62 V on the Co/PANI-PPYR catalyst. Figure 8(a) also shows that the ORR current density on the PANI-PPYR, Fe/PANI-PPYR and Fe-Co/PANI-PPYR catalysts presents a slow increment at the potential lower than their onset potentials, showing that the kinetic process of ORR on these catalysts hasn't been well improved in acidic media. Figure 8(b) indicates that all the prepared catalysts presented almost the same onset potential of ca. 0.09 V (vs. SCE) in alkaline solution. The diffusion current density of the ORR on the Co/PANI-PPYR in acidic and alkaline media is 4.3 mA/cm^2@0.2 V (vs. SCE) and 2.3 mA/cm^2@–0.3 V (vs. SCE), respectively. Figure 8 shows that the Co/PANI-PPYR catalyst presents lower onset potentials of ORR both in acidic and alkaline media than the Pt/C, while the diffusion current density of the ORR on the Co/PANI-PPYR is close to that on the Pt/C. The results show that Co-doped PANI-PPYR composite is an efficient electrocatalyst for ORR both in acidic and alkaline media. The low ORR electroactivity of the PANI-PPYR is ascribed to the absence of the transition metals like Fe and Co [15–19], although it presents the highest N content among the prepared catalysts. Co/PANI-PPYR and Fe/PANI-PPYR catalysts possess higher and almost the same nitrogen contents, and appropriate Co/Fe masses, resulting in the formation of more ORR active sites [21–23]. The highest ORR electroactivity of the Co/PANI-PPYR catalyst would be ascribed to its high Co content. Table 1 shows that the Fe-Co/PANI- PPYR catalyst exhibits low contents of nitrogen and metals (Fe and Co), which would be attributed to its low ORR electroactivity.

We further investigated the electrocatalytic activity of the prepared catalysts for ORR in detail. Polarization curves of the Co/PANI-PPYR catalyst as a typical sample at various rotating rates are shown in Figure 9. The Co/PANI-PPYR catalyst exhibits a well-defined limiting plateau in both acidic and alkaline media which implies that the ORR is diffusion-controlled below 0.4 V in acidic solution and below –0.3 V in alkaline solution. At higher potential (from 0.3 V to 0.5 V in H_2SO_4 solution or from –0.3 V to –0.15 V in NaOH solution), the ORR is under mixed diffusion-kinetic control. The 0.5–0.7 V range in H_2SO_4 solution or the –0.15–0.1 V range in NaOH solution corresponds to the ORR charge-transfer kinetic control.

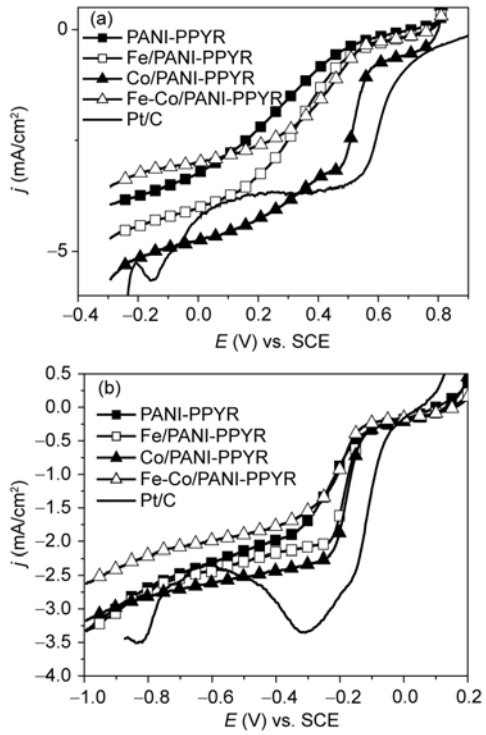

Figure 8 Polarization curves for oxygen reduction in O_2-saturated 0.5 mol/L H_2SO_4 (a) and O_2-saturated 1 mol/L NaOH (b) at a RDE modified with the prepared catalysts and Pt/C with a rotating rate of 800 r/min. Scan rate: 5 mV/s.

To further examine the ORR mechanism on the as-synthesized catalysts, the following Levich equation is used to describe the kinetics process of the ORR when the ORR mass-transport process in the solution becomes dominant:

$$j_d = 0.620n\,FD_0^{2/3}\omega^{1/2}\upsilon^{-1/6}C_0 \quad (1)$$

where j_d is the diffusion-limited current density for ORR, F is the Faraday constant, D_0 is the oxygen diffusion coefficient in 0.5 mol/L H_2SO_4 or 1 mol/L NaOH solution, ω is the rotation rate of the disk electrode, υ is the kinematic viscosity of 0.5 mol/L H_2SO_4 or 1 mol/L NaOH, C_0 is the concentration of O_2 in 0.5 mol/L H_2SO_4 or 1 mol/L NaOH at 25 °C. According to the slopes of the Levich plots for all catalysts (Figure 10), the n values for ORR are obtained and the results are shown in Figure 11. In 0.5 mol/L H_2SO_4 solution, the n values for ORR at PANI-PPYR, Fe/PANI-PPYR, Co/PANI-PPYR and Fe-Co/PANI-PPYR catalysts are 2.1, 3.6, 3.9 and 2.0, respectively. This shows that the electron transfer numbers of ORR on Co/PANI-PPYR and Fe/PANI-PPYR catalysts are close to 4, indicating a complete reduction of O_2 to H_2O. That is, a four-electron reaction of ORR is more favorable on Co/PANI-PPYR and Fe/PANI-PPYR catalysts than on PANI-PPYR and Fe-Co/PANI-PPYR catalysts. It can be reasonably considered that peroxides would be formed when the ORR takes

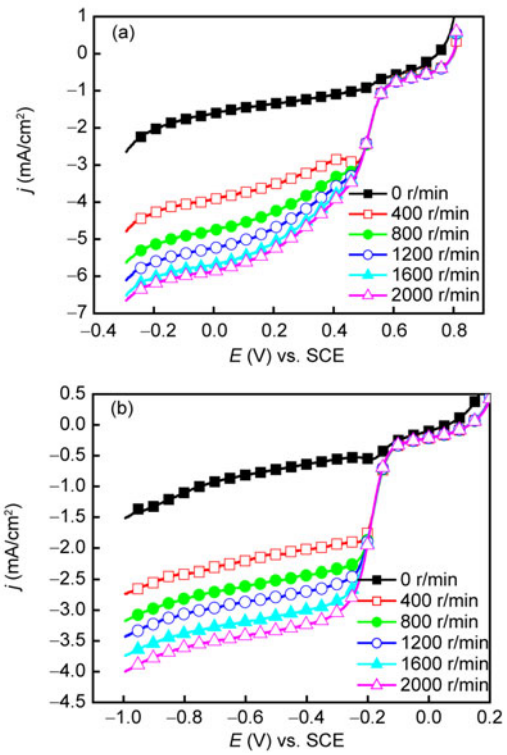

Figure 9 Polarization curves of the Co/PANI-PPYR catalyst at various rotating rates in O_2-saturated 0.5 mol/L H_2SO_4 (a) and O_2-saturated 1 mol/L NaOH (b). Scan rate: 5 mV/s.

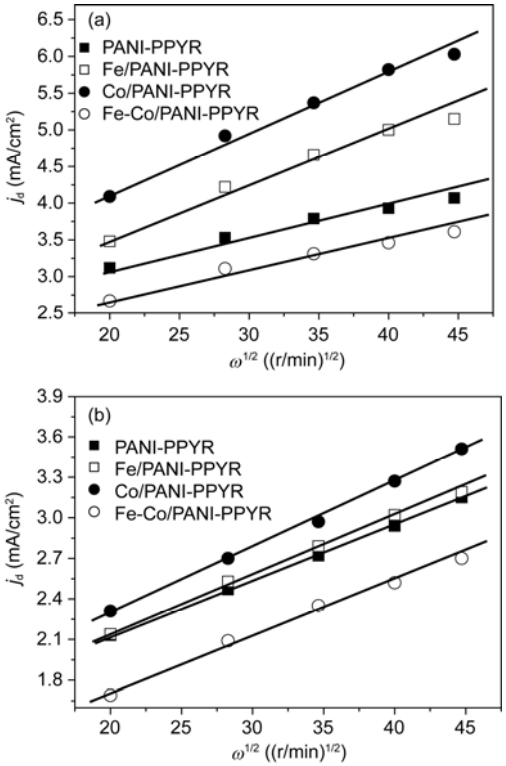

Figure 10 Levich plots for the ORR in O_2-saturated 0.5 mol/L H_2SO_4 (a) and O_2-saturated 1 mol/L NaOH (b) solution. Scan rate: 5 mV/s. Current density was measured at –0.1 V (vs. SCE) (a) and –0.7 V (vs. SCE) (b).

place on the PANI-PPYR and Fe-Co/ PANI-PPYR catalysts. Interestingly, the *n* values for ORR at all the four prepared catalysts in 1 mol/L NaOH solution are almost 3, indicating that both the complete reduction (4-electron mechanism) and partial reduction (2-electron mechanism) of O_2 are co-present in alkaline media. The results show that Co/PANI-PPYR and Fe/PANI-PPYR catalysts are suitable electrocatalysts for ORR in acidic solution.

The electrochemical stability of the Co/PANI-PPYR catalyst for ORR was investigated by using the long-term electrolysis test at a constant potential of 0.5 V in O_2-saturated 0.5 mol/L H_2SO_4 and −0.3 V in O_2-saturated 1 mol/L NaOH. As shown in Figure 12, the Co/PANI-PPYR catalyst shows a good stability with time either in acidic or alkaline solution, with the exception of the rapid decline of the ORR current density at the initial stage of electrolysis due to the speedy decrease of O_2 concentration near the catalyst surface. Experiments running for 2 h didn't show any obvious current density decay, showing the high electrocatalytic activity stability of the Co/PANI-PPYR for ORR. The stable ORR current density shown in Figure 12 indicates that the Co/PANI-PPYR catalyst would be a promising cathodic material applied to acidic or alkaline fuel cells.

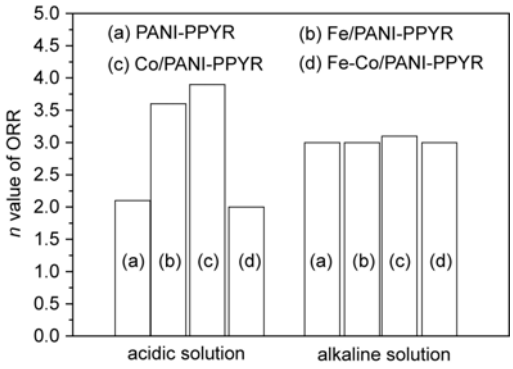

Figure 11 Electron transfer numbers (*n*) of ORR on various catalysts. The *n* numbers were calculated from the slope of Levich plots shown in Figure 10.

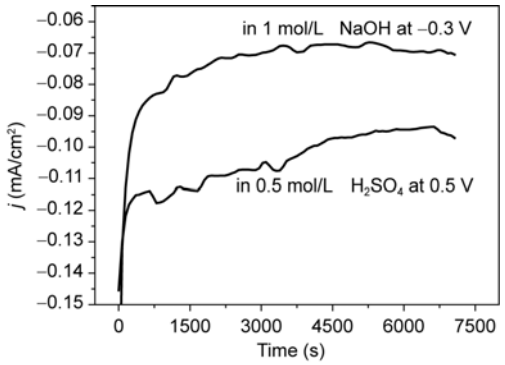

Figure 12 Chronoamperometric curves for the ORR catalyzed by the Co/PANI-PPYR catalyst in O_2-saturated 0.5 mol/L H_2SO_4 at 0.5 V and O_2-saturated 1 mol/L NaOH at −0.3 V, respectively. Potentials are referred to SCE.

4 Conclusions

In this work, a simple method has been proposed and used to prepare precious metal-free catalysts (PANI-PPYR, Fe/PANI-PPYR, Co/PANI-PPYR and Fe-Co/PANI-PPYR) with efficient ORR performance, using available and inexpensive polyaniline (PANI), polypyrrole (PPYR) and Fe/Co salts as precursors. We demonstrated that the addition of Co or Fe into the composite of PANI and PPYR plays a key role in the improvement of the ORR electroactivity of the metal-free PANI-PPYR catalyst while the co-addition of Fe and Co into the composite of PANI and PPYR leads to the decline of ORR activity. The catalysts of the present investigation can be easily obtained by calcining the PANI-PPYR composite or Fe/Co doped PANI-PPYR composites. All catalysts particles present a uniform distribution and porous structure. The ORR activity of the catalysts both in acidic and in alkaline media has been investigated by electrochemical voltammetry. Following conclusions have been drawn: (1) Fe/Co doped PANI-PPYR precursors were subjected to the high-temperature treatment to obtain the corresponding the Fe/Co doped C-N composites; (2) among the four as-synthesized catalysts, the Co/PANI-PPYR catalyst with the Co mass percentage of 4.22% shows the best performance of the ORR both in acidic and in alkaline media, with more positive onset potentials and large limiting-diffusion ORR current densities; (3) in acidic media, Co/PANI-PPYR and Fe/PANI-PPYR catalysts catalyze the ORR via a four-electron transfer process while PANI-PPYR and Fe-Co/PANI-PPYR catalysts catalyze the ORR via a two-electron transfer process, however, in alkaline media, a three-electron transfer process for the ORR was found on all as-synthesized catalysts; (4) the co-doped Fe and Co into the PANI-PPYR composite, leading to the synthesis of Fe-Co/PANI-PPYR catalyst, presents low electroactivity for ORR both in acidic and in alkaline media, further study on the effect of the doped metals on the ORR electroactivity is being under way in our group; (5) the as-synthesized Co/PANI-PPYR catalyst shows good electroactivity stability for ORR both in acidic and in alkaline media, no obvious ORR current decay was observed after 2 h electrolysis at a constant potential.

This work was supported by the National Natural Science Foundation of China (21376070, 20876038), the Scientific Research Fund of Hunan Provincial Education Department (11K023), and Hunan Provincial Natural Science Foundation of China (14JJ2096).

1 Jasinski R. A new fuel cell cathode catalyst. *Nature*, 1964, 201: 1212–1213

2 (a) Bashyam R, Zelenay P. A class of non-precious metal composite catalysts. *Nature*, 2006, 443: 63–66; (b) Egli M, Pallan PS. Insights

from crystallographic studies into the structural and pairing properties of nucleic acid analogs and chemically modified DNA and RNA oligonucleotides. *Annu Rev Biophys Biomol Struct*, 2007, 36: 281–305
3 Seeliger W, Hamnett A. Novel electrocatalysts for oxygen reduction. *Electrochim Acta*, 1992, 37: 763–765
4 Jahnke H, Schonbron M, Zimmerman G. *Organic Dyestuffs as Catalysts for Fuel Cells*, *Physical and Chemical Applications of Dyestuffs. Topics in Current Chemistry*. Berlin：Springer Berlin/Heidelberg，1976. 165–168
5 Zhong H, Zhang H, Liu G, Liang Y, Hu J, Yi B. A novel non-noble electrocatalyst for PEM fuel cell based on molybdenum nitride. *Electrochem Commun*, 2006, 8: 707–712
6 Ishihara A, Lee K, Doi S, Mitsushima S, Kamiya N, Hara M, Domen K, Fukuda K, Ota K-ichiro. Tantalum oxynitride for a novel cathode of PEFC. *Electrochem Solid-State Lett*, 2005, 8: A201–A203
7 Liu G, Zhang HM, Wang MR, Zhong HX, Chen J. Preparation characterization of ZrO_xN_y–C and its application in PEMFC as an electrocatalyst for oxygen reduction. *J Power Sources*, 2007, 172: 503–510
8 Biddinger EJ, Ozkan US. Methanol tolerance of CN_x oxygen reduction catalysts. *Top Catal*, 2007, 46: 339–348
9 Liu G, Li X, Ganesan P, Popov BN. Development of non-preciousmetal oxygen-reduction catalysts for PEM fuel cells based on N-doped ordered porous carbon. *Appl Catal B*: *Environ*, 2009, 93: 156–165
10 Lei M, Li PG, Li LH, Tang WH. A highly ordered Fe-N-C nanoarray as a non-precious oxygen-reduction catalyst for proton exchange membrane fuel cells. *J Power Sources*, 2011, 196: 3548–3552
11 Deng L, Zhou M, Liu C, Liu L, Liu C, Dong S. Development of high performance of Co/Fe/N/CNT nanocatalyst for oxygen reduction in microbial fuel cells. *Talanta*, 2010, 81: 444–448
12 Byon HR, Suntivich J, Crumlin EJ, Shao-Horn Y. Fe-N-modified multi-walled carbon nanotubes for oxygen reduction reaction in acid. *Phys Chem Chem Phys*, 2011, 13: 21437–21445
13 Morozan A, Jegou P, Jousselme B, Palacin S. Electrochemical performance of annealed cobalt-benzotriazole/CNTs catalysts towards the oxygen reduction reaction. *Phys Chem Chem Phys*, 2011, 13: 21600–21607
14 Wu G, More KL, Johnston CM, Zelenay P. High-performance electrocatalysts for oxygen reduction derived from polyaniline, iron, and cobalt. *Science*, 2011, 332: 443–447
15 Subramanian NP, Kumaraguru SP, Colon-Mercado H, Kim H, Popov BN, Black T, Chen DA. Studies on Co-based catalysts supported on modified carbon substrates for PEMFC cathodes. *J Power Sources*, 2006, 157: 56–63
16 Lalande G, Côté R, Guay D, Dodelet JP, Weng LT, Bertrand P. Is nitrogen important in the formulation of Fe-based catalysts for oxygen reduction in solid polymer fuel cells? *Electrochim Acta*, 1997, 42: 1379–1388
17 Gojkovic SLJ, Gupta S, Savinell RF. Heat-treated iron (III) tetramethoxyphenyl porphyrin chloride supported on high-area carbon as an electrocatalyst for oxygen reduction. Part II. Kinetics of oxygen reduction. *J Electroanal Chem*, 1999, 462: 63–72
18 Faubert G, Côté R, Guay D, Dodelet JP, Dénès G, Bertrandc P. Iron catalysts prepared by high-temperature pyrolysis of tetraphenylporphyrins adsorbed on carbon black for oxygen reduction in polymer electrolyte fuel cells. *Electrochim Acta*, 1998, 43: 341–353
19 Lefevre M, Dodelet JP. O_2 reduction in PEM fuel cells: Activity and active site structural information for catalysts otained by the pyrolysis at high temperature of Fe precursors. *J Phys Chem B*, 2000, 104: 11238–11247
20 Wu G, Nelson M, Ma S, Meng H, Cui G, Shen PK. Synthesis of nitrogen-doped onion-like carbon and its use in carbon-based CoFe binary non-precious-metal catalysts for oxygen-reduction. *Carbon*, 2011, 49: 3972–3982
21 Nallathambi V, Lee J-W, Kumaraguru SP, Wu G, Popov BN. Development of high performance carbon composite catalyst for oxygen reduction reaction in PEM proton exchange membrane fuel cells. *J Power Sources*, 2008, 183: 34–42
22 Lefèvre M, Proietti E, Jaouen F, Dodelet JP. Iron-based catalysts with improved oxygen reduction activity in polymer electrolyte fuel cells. *Science*, 2009, 324: 71–74
23 Pylypenko S, Mukherjee S, Olson TS, Atanassov P. Non-platinum oxygen reduction electrocatalysts based on pyrolyzed transition metal macrocycles. *Electrochim Acta*, 2008, 53: 7875–7883